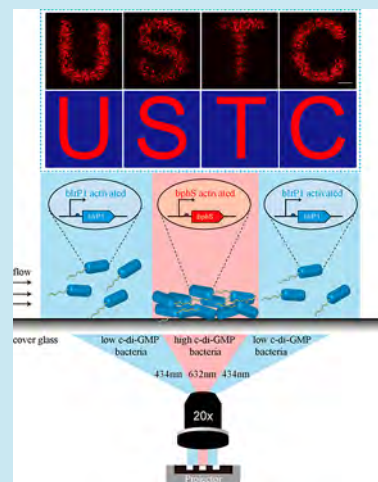


Bioprinting Living Biofilms through Optogenetic Manipulation

Yajia Huang,^{†,§} Aiguo Xia,^{‡,§} Guang Yang,^{*,†} and Fan Jin^{*,‡}[†]Department of Biomedical Engineering, College of Life Science and Technology, Huazhong University of Science and Technology, Wuhan 430074, PR China[‡]Hefei National Laboratory for Physical Sciences at the Microscale, Department of Polymer Science and Engineering, CAS Key Laboratory of Soft Matter Chemistry, University of Science and Technology of China, Hefei 230026, PR China

Supporting Information

ABSTRACT: In this paper, we present a new strategy for microprinting dense bacterial communities with a prescribed organization on a substrate. Unlike conventional bioprinting techniques that require bioinks, through optogenetic manipulation, we directly manipulated the behaviors of *Pseudomonas aeruginosa* to allow these living bacteria to autonomously form patterned biofilms following prescribed illumination. The results showed that through optogenetic manipulation, patterned bacterial communities with high spatial resolution (approximately 10 μm) could be constructed in 6 h. Thus, optogenetic manipulation greatly increases the range of available bioprinting techniques.



KEYWORDS: bioprinting, optogenetic manipulation, bacterial biofilms, *Pseudomonas aeruginosa*

Bioprinting is an increasingly applied technique that facilitates the precise placement of biologics,^{1,2} such as living cells, DNA, proteins, and growth factors, for the computer-aided fabrication of biologically active materials with a prescribed organization. Bioprinting offers unprecedented opportunities to precisely fabricate biologically active materials, in which bioprinting of living mammalian cells largely received attention because it can be applied in various fields, including tissue engineering and regenerative medicine,³ transplantation and clinics, drug discovery,⁴ and cancer research.⁵ The living style of bacteria is quite different with mammalian cells, where bacteria favor forming dense bacterial communities, known as biofilms, to survive and thrive in almost any ecological niche.⁶ It is well established that living biofilms are able to produce functional biopolymers and degrade different organic compounds during their growth.⁷ For example, *Bacillus subtilis* produce and secrete amyloid fibers that facilitate and support their adhesion on the air/water interface to form biofilms.⁸ Similarly, *Acetobacter xylinum* produce the bacterial cellulose at the air/water interface during the biofilms formation,⁹ in which bacterial cellulose has been shown to be a good candidate for fabricating of medical implants,^{10,11} such as ear transplants, artificial skins and potential blood vessels. Biofilms formed by *Pseudomonas putida* are able to degrade organic compounds,¹² such as phenol, toluene and benzene, and thus have been applied to treat

industrial wastewater.¹³ In light of these unique and attractive traits arising from living biofilms, bioprinting of living biofilms with a prescribed organization to create bacteria-derived functional materials has gained much attention.^{14–16} Most recently, using 3D printing of *P. putida* or *A. xylinum*, Schaffner *et al.* have created two types of “living materials” to demonstrate that these materials embedded with living bacteria can degrade pollutants or produce medically relevant materials.¹⁷

To maintain cell growth and support 3D architectures in those printing materials, hydrogels with good biocompatibility and matching viscoelasticity, known as bioink, are typically required to fabricate the shaped scaffolds.¹⁸ It has been known that cells in biofilms live in a self-produced 3D polymer network of extracellular polymeric substances (EPS) that mainly include polysaccharides, proteins and nucleic acids, in which the self-produced matrix can protect cells and maintain the structure of biofilms.⁷ It is thereby reasoned that the self-produced EPS is good to use as bioink for the printing of living bacteria. In addition, EPS production and biofilm formation are tightly regulated by the second messenger cyclic dimeric guanosine monophosphate (c-di-GMP) in almost bacteria.¹⁹ These traits arising bacterial EPS inspire us to develop a bioink-

Received: January 2, 2018

Published: April 17, 2018

free strategy to print dense bacterial communities on a substrate without using additive manufacturing or additional surface modification. Using a combination of optogenetic tools and microprojection, here, we directly manipulate the c-di-GMP levels in single *Pseudomonas aeruginosa* cells (a model microorganism for biofilm-related studies), which allow these living cells to form patterned biofilms following prescribed illumination. Our results demonstrated that patterned bacterial communities with high spatial resolution (approximately 10 μm) can be constructed in 6 h through optogenetic manipulation.

RESULTS

Manipulation of c-di-GMP Levels of Engineered Strain via Optogenetic Tools. In our proposed strategy, we first incorporated two optogenetic modules into the chromosome of *P. aeruginosa* by using the mini-CTX and mini-Tn7 systems.^{20,21} These optogenetic modules comprise two light-responsive parts (Figure 1a): the first part encodes a heme

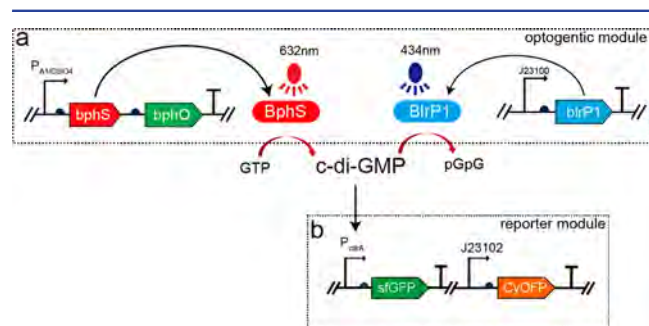


Figure 1. Schematic showing the optogenetic and reporter module in the engineered strain used in our bioprinting: (a) optogenetic module, (b) reporter module.

oxygenase (*bphO*) and a c-di-GMP diguanylate cyclase (*bphS*) that can cyclize two guanosine triphosphate (GTP) molecules to form a c-di-GMP molecule in the presence of near-infrared light.²² The second part encodes a c-di-GMP phosphodiesterase (*blrP1*) that can hydrolyze c-di-GMP in the presence of blue light.²³ Therefore, these optogenetic modules enable the precise manipulation of the c-di-GMP levels in *P. aeruginosa* through dual-color illumination. The c-di-GMP levels control motility, biofilm formation, extracellular polymeric substance production, and antibiotic resistance in the bacteria.^{24,25} We therefore expected that biofilm formation by *P. aeruginosa* could be controlled through optogenetic manipulation of the c-di-GMP levels. To monitor the c-di-GMP levels in the optogenetic strains, we also inducted a plasmid harboring a c-di-GMP level reporter module into the strain.²⁶ The reporter module encodes two fluorescent proteins with different colors:²⁷ a green fluorescent protein (sfGFP) expressed using a c-di-GMP regulatory promoter (*P_{cdtA}*) and an orange fluorescent protein (CyOFF1) expressed using a constitutive promoter (J23102) (Figure 1b). Thus, we could monitor the c-di-GMP levels in the bacteria by using the fluorescent intensities ratio of sfGFP and CyOFF1.

Optimization of Bioprinting Conditions. We microprinted *P. aeruginosa* on a cover glass by using a standard flow cell system that has widely been used to continuously culture biofilms (Figure 2a and Figure S1).²⁸ The flowing culture readily allows the cells with lower c-di-GMP levels to detach from the cover glass to the bulk medium,²⁹ and these detached

cells are eventually washed out by the flow. The prescribed illuminations, including the red light (632 nm) and blue light (434 nm), were projected onto the cover glass by using a digital micromirror device-based (DMD) light-emitting diode (LED) projector through a 20 \times oil objective. Consequently, several printing conditions, including illumination power density, inoculation cell density, circulating rate and nutrient availability, are expected to affect the biofilm formation in the flow chamber, which would thus in turn affect the microprinting process. To find the appropriate conditions for the printing, first, we microprojected the letter “T” and varied illumination power density of red- and blue light to find appropriate illuminations that can lead cells to form a “T” pattern (Figure S2a–d and S3a–e) and do not affect cell growth (Figure S4b), where red light was projected onto the letter, while blue light was projected onto the complementary areas. We found that the illumination of red light (632 nm) and blue light (434 nm) with the power density of 10.1 $\mu\text{W cm}^{-2}$ and 6.4 $\mu\text{W cm}^{-2}$ is an appropriate condition that allows cells to quickly form the “T”-patterned bacterial communities (Figure S5). In addition, we found that the dual-color responsive strain (PAO1-*bphS*-*blrP1*-reporter) can form a complete “T”-pattern, while the monochrome responsive strain (PAO1-*bphS*-reporter) cannot form the pattern. Interestingly, the “T” pattern can be barely observed in the sfGFP channel because red illumination increased c-di-GMP levels in the region (Figure S2e). Furthermore, we found that inverting the projection of red- and blue light led dual-color responsive strain to form bacterial communities with an inverted pattern (Figure S4a). These results indicated that the pattern formed by bacterial communities can be fully controlled via dual-color optogenetic manipulations of c-di-GMP levels. It should be emphasized that the currently used illuminations do not affect the biofilm formation of wild-type strain (Figure S4b).

Next, we inoculated different amount of cells at the beginning and illuminated them with the optimized illuminations to find an appropriate inoculation density that can lead the “T”-pattern to form as quick as possible. We found that the inoculation of 4.8×10^6 or 1.3×10^6 cells per square centimeter at the beginning led the “T”-patterned bacterial communities to quickly form within 6 h (Figure S6a,b), and the lesser inoculation density (7.0×10^5 cell cm^{-2}) delayed the “T”-pattern to form (Figure S6c). Also we varied the circulating rate in the flow chamber or used relative unfavorable (succinate) instead of favorable carbon source (glutamate), in which these culturing conditions have been shown to affect biofilms formation.^{30,31} We found that increasing the circulating rate from 3 to 5 mL h^{-1} (Figure S7a,b) did not affect the “T”-pattern to form, but succinate feeding delayed the “T”-pattern to form (Figure S7c).

Bioprinting Living *P. aeruginosa* Biofilms Using Optimized Conditions. Using these optimized printing conditions, we microprojected the four letters “USTC” (the abbreviation for the University of Science and Technology of China) onto the cover glass to demonstrate the microprinting of living biofilms. The color maps shown in Figure S5 indicated the averaged illumination densities during microprinting. As shown in Figure 2c and Movie S1, cells could self-organize to form dense bacterial communities in the regions illuminated by red light after 6 h, and they eventually formed multilayered biofilms with a prescribed organization in 20 h (Figure 2d and Movie S2). To quantify the bacterial behaviors during microprinting, we assessed the averaged bacterial densities

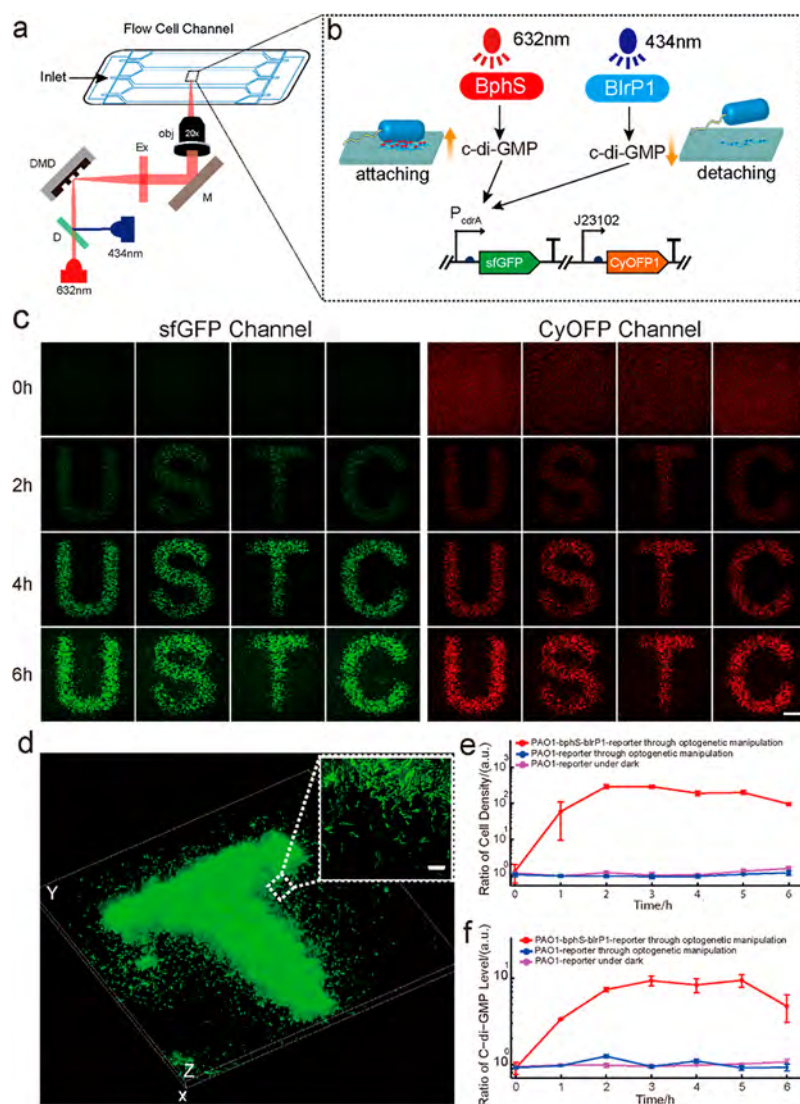


Figure 2. Bioprinting living *P. aeruginosa* biofilms through optogenetic manipulation. (a) Schematic shows the setup used in the bioprinting, (b) where 632 nm illuminations elevate the c-di-GMP level that allows cells to attach to the surface, whereas 434 nm illuminations decrease the c-di-GMP level that allows cells to detach from the surface. (c) Representative fluorescent images show that the strain PAO1-*bphS-blrP1*-reporter self-organized to form patterned bacterial communities illuminated with prescribed patterns of “U” “S” “T” “C” by using a digital micromirror DMD LED projector during 6 h, where the images with green or red color represent the images arising from sfGFP or CyOFP1 channel, respectively. (d) 3D reconstructed image shows the successful bioprinting of living *P. aeruginosa* biofilms according to the prescribed illumination of “T”. (e) Time dependence of the ratio of (e) bacterial densities or (f) c-di-GMP levels in the red- and blue-illuminated regions using the strain PAO1-*bphS-blrP1*-reporter (red symbols and line) or PAO1-reporter (wild-type, blue symbols and line, where magenta symbols and line represent the strain PAO1-reporter under a dark condition); error bars are the std. from 3 replicates. Scale bar in panel c or d is 100 or 10 μm , respectively.

and averaged c-di-GMP levels in cells in the region illuminated by red and blue light. We observed that cells quickly responded to red illumination and self-organized in the red-illuminated region at first 2 h, as indicated by the ratio of bacterial densities in the red- and blue-illuminated regions, which markedly increased up to 300 folds (red symbols and line, Figure 2e). In addition, we observed that the c-di-GMP levels in cells also increased in the red-illumination region at first 2 h, as indicated by the ratio of the c-di-GMP levels in the red- and blue-illuminated regions, which increased up to 10 folds (red symbols and line, Figure 2f). By contrast, the treatments of wild-type cells with identical conditions or in the absence of illumination (dark condition) led the ratio of bacterial densities (blue symbols and line, Figure 2e) or the ratio of the c-di-GMP levels (blue symbols and line, Figure 2f) to remain a constant.

We noticed slight decrease in the ratio of bacterial densities or the c-di-GMP levels in the red- and blue-illuminated regions after 5 h (Figure 2e and f). This is because bacterial growth in the red-illuminated region eventually caused some cells to be dispersed across the region.

To test the feasibility that erasing of patterned bacterial communities, first, we manipulated cells to form a “T”-pattern at first 2 h (Figure 3a). Then, we turned off the red light and illuminated those cells by using blue light ($6.4 \mu\text{W cm}^{-2}$) in the presence at entire field. We found that the “T”-pattern gradually dispersed in the following 6 h (Figure 3a and c) accompanied by the decrease in c-di-GMP levels (Figure 3b). The results conclusively demonstrate that formation or dispersion of patterned bacterial communities can be fully controlled *via* the manipulation of c-di-GMP levels.

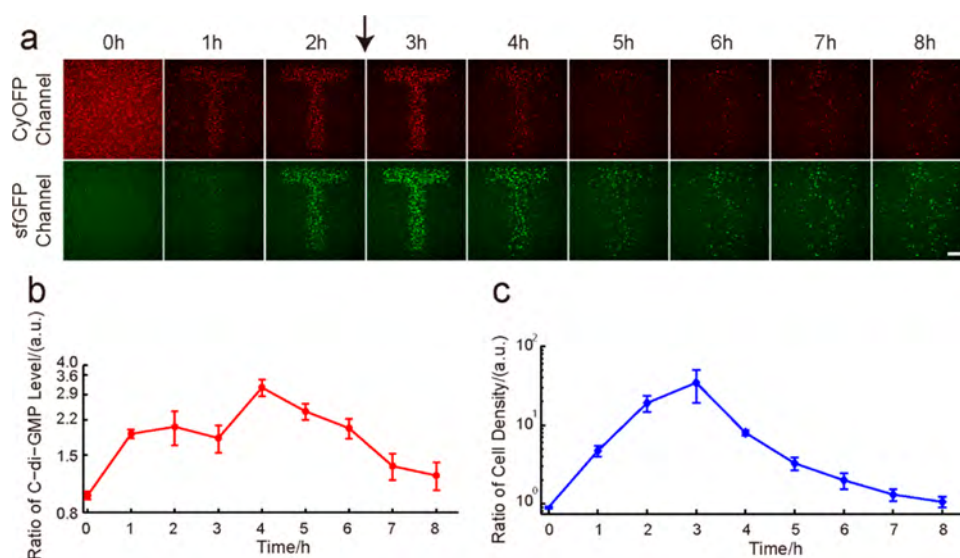


Figure 3. Erasing the pattern formed by *P. aeruginosa* through optogenetic manipulation. (a) Representative fluorescent images show that blue-illuminations ($6.4 \mu\text{W cm}^{-2}$, entire field after 2 h) lead the “T”-pattern formed by PAO1-*bphS-blrP1*-reporter cells to disperse in following 6 h, where the printing illuminations (red: $10.1 \mu\text{W cm}^{-2}$, blue: $6.4 \mu\text{W cm}^{-2}$) were used to lead cell to form the “T”-pattern at first 2 h; the black arrow represents the time point that blue-illuminations in the entire field was applied. The images with green or red color represent the images arising from sfGFP or CyOFF1 channel, respectively. (b) Time dependence of the ratio of (b) bacterial densities or (c) c-di-GMP levels in the red- and blue-illuminated regions, where error bars are the std. from 3 replicates. Scale bar is $100 \mu\text{m}$.

DISCUSSION

In summary, we demonstrated that the optogenetic manipulation of c-di-GMP levels in single *P. aeruginosa* cells can be applied to construct patterned biofilms on a substrate. This method can be applied for construction of bacteria-derived functional materials by printing engineered *P. putida* or *A. xylinum*, because c-di-GMP is a key second messenger in the decision between the motile planktonic and sessile biofilm-associated cells.^{32,33} Furthermore, this strategy can be readily expanded to print living mammalian cells through the incorporation of an optogenetic module that allows cells to secrete adhesion proteins (cell glue) in the presence of light. In addition to creating functional “living-materials”, construction of patterned biofilms would provide an opportunity to the fundamental research of biofilm-related studies, including biofilms formation, biofilms dispersion and cell singling in biofilms. This is because the spatial organization of biofilms are expected to affect cell signaling,⁶ metabolic activity, and cell differentiation,³⁴ which in turn affects biofilm functionalities.³⁵ For example, Connell *et al.* uncovered how spatial organization and bacterial aggregate size affect the quorum sensing signaling in *P. aeruginosa* using the microprinting of living biofilms.¹⁶

Bioprinting through optogenetic manipulation offers unique advantages: (i) it does not require bioink or the addition of other chemical reagents; (ii) it provides a self-produced EPS matrix to accommodate these living bacteria, ensuring that the function of biofilms would not be affected; and (iii) the light intensity required for bioprinting is sufficiently weak; thus, the printing process does not affect the activity of living cells. However, the following disadvantages limit the extent to which optogenetic manipulation can be used in bioprinting: (i) it requires additional gene manipulation for living cells, and (ii) it requires a longer printing time to form mature biofilm. We cannot precisely control the three-dimensional structures of printed biofilms by using the current illumination method, but multiphoton illumination may overcome this limitation.

METHODS

Plasmids, Strains and Growth Conditions. Bacterial strains and plasmids used in this study are listed in Table S1. Additional details for construction of the optogenetic and reporter strains are given in Supplementary Methods. Strains were grown on LB agar plates at $37 \text{ }^\circ\text{C}$ for 24 h. Monoclonal colonies were inoculated and cultured with a minimal medium (FAB) at $37 \text{ }^\circ\text{C}$ with 30 mM sodium glutamate (or sodium succinate used in control experiment) as carbon source under an aerobic condition, in which the culture medium contains following compositions per liter: $(\text{NH}_4)_2\text{SO}_4$, 2 g; $\text{Na}_2\text{HPO}_4 \cdot 12\text{H}_2\text{O}$, 12.02 g; KH_2PO_4 , 3 g; NaCl, 3 g; MgCl_2 , 93 mg; $\text{CaCl}_2 \cdot 2\text{H}_2\text{O}$, 14 mg; FeCl_3 , 1 μmol ; and trace metals solution ($\text{CaSO}_4 \cdot 2\text{H}_2\text{O}$, 200 mg L^{-1} ; $\text{MnSO}_4 \cdot 7\text{H}_2\text{O}$, 200 mg L^{-1} ; $\text{CuSO}_4 \cdot 5\text{H}_2\text{O}$, 20 mg L^{-1} ; $\text{ZnSO}_4 \cdot 7\text{H}_2\text{O}$, 20 mg L^{-1} ; $\text{CoSO}_4 \cdot 7\text{H}_2\text{O}$, 10 mg L^{-1} ; $\text{NaMoO}_4 \cdot \text{H}_2\text{O}$, 10 mg L^{-1} ; H_3BO_3 , 5 mg L^{-1}), 1 mL. The strains were harvested at $\text{OD}_{600} = 2.0$, and the bacterial cultures were further diluted (1:100) in fresh FAB mediums with $30 \mu\text{g} \cdot \text{mL}^{-1}$ gentamycin to culture until $\text{OD}_{600} = 0.6$ before used.

Bioprinting Living Biofilms. Bacterial strain was inoculated into a flow cell (Denmark Technical University) and continuously cultured at $26.0 \pm 0.1 \text{ }^\circ\text{C}$ by flowing FAB medium (3.0 mL h^{-1}) (Figure S1). The invert fluorescent microscope (Olympus, IX71) equipped with a 20 \times oil objective and a sCMOS camera (Zyla 4.2 Andor) was used to collect fluorescent images with 1/1800 frame per second. sfGFP and CyOFF1 were excited using a 480 nm light (ThorLabs) and imaged using single-band emission filters (Semrock): sfGFP (520/28 nm) or CyOFF1 (583/22 nm). The c-di-GMP levels in single cells were determined using the ratio of sfGFP and CyOFF1 intensities. The manipulation light of 632 nm (Lumencor) or 434 nm (Lumencor) with a prescribed pattern (Figure S5) was projected on the surface where the bacteria attached through a DMD projector (Mosaic Andor) and the oil objective. The illumination density of manipulation lights was determined by measuring the power at outlet of the oil

objective using a power meter (Newport 842-PE). The living bacteria (here the strain PAO1-bphS-blrP1 used) were allowed to continuously grow in the flow chamber for 20 h in the presence of the manipulation lights to form multilayer biofilm. Afterward, the 20-h old biofilm was stained using SYTO 9 (Life Technologies) and then was imaged using a spinning-disc confocal microscope (Revolution Andor) equipped with a 100× oil objective and an EMCCD (iX897 Andor). A multifield (8 × 8) and z-scanning (0.5 μm per step) confocal images were acquired to reconstruct the three-dimensional structure of biofilm.

Data Analysis. Cell density in the region illuminated by red or blue light was evaluated using the ratio of fluorescent intensities arising from CyOFPI at the region and the area occupied by the cells at the corresponding region. A general image processing algorithm coded by MATLAB was used to analyze the fluorescent intensities arising from CyOFPI or arising from sfGFP and areas occupied by the cells at the red or blue-illuminated region. The c-di-GMP levels in cells located at the red- or blue-illuminated region were determined using the ratio of sfGFP and CyOFPI.

■ ASSOCIATED CONTENT

Supporting Information

The Supporting Information is available free of charge on the ACS Publications website at DOI: 10.1021/acssynbio.8b00003.

Additional Methods; Figures S1–S7; Table S1 (PDF)
Movie S1 (AVI)
Movie S2 (AVI)

■ AUTHOR INFORMATION

Corresponding Authors

*E-mail: yang_sunny@yahoo.com.

*E-mail: fjinustc@ustc.edu.cn.

ORCID

Guang Yang: 0000-0001-9198-3556

Fan Jin: 0000-0003-2313-0388

Author Contributions

[§]Y.H. and A.X. contributed equally to this work. F.J. conceived the project. Y.J.H. and A.G.X. performed the experiments. Y.J.H., F.J. and G.Y. contributed jointly to data interpretation and manuscript preparation. All authors reviewed the manuscript.

Notes

The authors declare no competing financial interest.

■ ACKNOWLEDGMENTS

We thank Dr. M. Gomelsky, who provided the optogenetic plasmid. This work was supported by the National Natural Science Foundation of China [21774117, 21474098, 21274141, and 21522406] and the Fundamental Research Funds for the Central Universities [WK2340000066 and WK2030020023], where Yajia Huang and Guang Yang were supported by the National Natural Science Foundation of China [31270150 and 21774039].

■ REFERENCES

- (1) Chia, H. N., and Wu, B. M. (2015) Recent advances in 3D printing of biomaterials. *J. Biol. Eng.* 9, 4.
- (2) Włodarczyk-Biegun, M. K., and del Campo, A. (2017) 3D bioprinting of structural proteins. *Biomaterials* 134, 180–201.
- (3) Gomes, M. E., Rodrigues, M. T., Domingues, R. M., and Reis, R. L. (2017) Tissue Engineering and Regenerative Medicine: New

Trends and Directions—A Year in Review. *Tissue Eng., Part B* 23, 211–224.

(4) Peng, W., Datta, P., Ayan, B., Ozbolat, V., Sosnoski, D., and Ozbolat, I. T. (2017) 3D bioprinting for drug discovery and development in pharmaceuticals. *Acta Biomater.* 57, 26–46.

(5) Zhang, Y. S., Duchamp, M., Oklu, R., Ellisen, L. W., Langer, R., and Khademhosseini, A. (2016) Bioprinting the cancer microenvironment. *ACS Biomater. Sci. Eng.* 2, 1710–1721.

(6) Flemming, H.-C., Wingender, J., Szewzyk, U., Steinberg, P., Rice, S. A., and Kjelleberg, S. (2016) Biofilms: an emergent form of bacterial life. *Nat. Rev. Microbiol.* 14, 563.

(7) Flemming, H.-C., and Wingender, J. (2010) The biofilm matrix. *Nat. Rev. Microbiol.* 8, 623–633.

(8) Vlamakis, H., Chai, Y., Beaugrand, P., Losick, R., and Kolter, R. (2013) Sticking together: building a biofilm the *Bacillus subtilis* way. *Nat. Rev. Microbiol.* 11, 157.

(9) Brown, R. M., Willison, J., and Richardson, C. L. (1976) Cellulose biosynthesis in *Acetobacter xylinum*: visualization of the site of synthesis and direct measurement of the in vivo process. *Proc. Natl. Acad. Sci. U. S. A.* 73, 4565–4569.

(10) Czaja, W. K., Young, D. J., Kawecki, M., and Brown, R. M. (2007) The future prospects of microbial cellulose in biomedical applications. *Biomacromolecules* 8, 1–12.

(11) Sulaeva, I., Henniges, U., Rosenau, T., and Potthast, A. (2015) Bacterial cellulose as a material for wound treatment: Properties and modifications. A review. *Biotechnol. Adv.* 33, 1547–1571.

(12) Gonzalez, G., Herrera, G., Garcia, M. T., and Pena, M. (2001) Biodegradation of phenolic industrial wastewater in a fluidized bed bioreactor with immobilized cells of *Pseudomonas putida*. *Bioresour. Technol.* 80, 137–142.

(13) Samanta, S. K., Singh, O. V., and Jain, R. K. (2002) Polycyclic aromatic hydrocarbons: environmental pollution and bioremediation. *Trends Biotechnol.* 20, 243–248.

(14) Timm, C. M., Hansen, R. R., Doktycz, M. J., Retterer, S. T., and Pelletier, D. A. (2015) Microstencils to generate defined, multi-species patterns of bacteria. *Biomicrofluidics* 9, 064103.

(15) Aznaveh, N. B., Safdar, M., Wolfaardt, G., and Greener, J. (2014) Micropatterned biofilm formations by laminar flow-templating. *Lab Chip* 14, 2666–2672.

(16) Connell, J. L., Kim, J., Shear, J. B., Bard, A. J., and Whiteley, M. (2014) Real-time monitoring of quorum sensing in 3D-printed bacterial aggregates using scanning electrochemical microscopy. *Proc. Natl. Acad. Sci. U. S. A.* 111, 18255–18260.

(17) Schaffner, M., Rühs, P. A., Coulter, F., Kilcher, S., and Studart, A. R. (2017) 3D printing of bacteria into functional complex materials. *Sci. Adv.* 3, ea06804.

(18) Malda, J., Visser, J., Melchels, F. P., Jüngst, T., Hennink, W. E., Dhert, W. J., Groll, J., and Huttmacher, D. W. (2013) 25th anniversary article: engineering hydrogels for biofabrication. *Adv. Mater.* 25, 5011–5028.

(19) Hengge, R. (2009) Principles of c-di-GMP signalling in bacteria. *Nat. Rev. Microbiol.* 7, 263.

(20) Hoang, T. T., Kutchma, A. J., Becher, A., and Schweizer, H. P. (2000) Integration-proficient plasmids for *Pseudomonas aeruginosa*: site-specific integration and use for engineering of reporter and expression strains. *Plasmid* 43, 59–72.

(21) Choi, K.-H., and Schweizer, H. P. (2006) mini-Tn7 insertion in bacteria with single attTn7 sites: example *Pseudomonas aeruginosa*. *Nat. Protoc.* 1, 153.

(22) Ryu, M.-H., and Gomelsky, M. (2014) Near-infrared light responsive synthetic c-di-GMP module for optogenetic applications. *ACS Synth. Biol.* 3, 802–810.

(23) Barends, T. R., Hartmann, E., Griese, J. J., Beitlich, T., Kirienko, N. V., Ryjenkov, D. A., Reinstein, J., Shoeman, R. L., Gomelsky, M., and Schlichting, I. (2009) Structure and mechanism of a bacterial light-regulated cyclic nucleotide phosphodiesterase. *Nature* 459, 1015.

(24) Jenal, U., Reinders, A., and Lori, C. (2017) Cyclic di-GMP: second messenger extraordinaire. *Nat. Rev. Microbiol.* 15, 271.

- (25) Schirmer, T., and Jenal, U. (2009) Structural and mechanistic determinants of c-di-GMP signalling. *Nat. Rev. Microbiol.* 7, 724.
- (26) Rybtke, M. T., Borlee, B. R., Murakami, K., Irie, Y., Hentzer, M., Nielsen, T. E., Givskov, M., Parsek, M. R., and Tolker-Nielsen, T. (2012) Fluorescence-based reporter for gauging cyclic di-GMP levels in *Pseudomonas aeruginosa*. *Appl. Environ. Microbiol.* 78, 5060–5069.
- (27) Chu, J., Oh, Y., Sens, A., Ataie, N., Dana, H., Macklin, J. J., Laviv, T., Welf, E. S., Dean, K. M., and Zhang, F. (2016) A bright cyan-excitable orange fluorescent protein facilitates dual-emission microscopy and enhances bioluminescence imaging in vivo. *Nat. Biotechnol.* 34, 760.
- (28) Heydorn, A., Ersbøll, B. K., Hentzer, M., Parsek, M. R., Givskov, M., and Molin, S. (2000) Experimental reproducibility in flow-chamber biofilms. *Microbiology* 146, 2409–2415.
- (29) Gibiansky, M. L., Conrad, J. C., Jin, F., Gordon, V. D., Motto, D. A., Mathewson, M. A., Stopka, W. G., Zelasko, D. C., Shrout, J. D., and Wong, G. C. (2010) Bacteria use type IV pili to walk upright and detach from surfaces. *Science* 330, 197–197.
- (30) Shrout, J. D., Chopp, D. L., Just, C. L., Hentzer, M., Givskov, M., and Parsek, M. R. (2006) The impact of quorum sensing and swarming motility on *Pseudomonas aeruginosa* biofilm formation is nutritionally conditional. *Mol. Microbiol.* 62, 1264–1277.
- (31) Salek, M. M., Jones, S. M., and Martinuzzi, R. J. (2009) The influence of flow cell geometry related shear stresses on the distribution, structure and susceptibility of *Pseudomonas aeruginosa* 01 biofilms. *Biofouling* 25, 711–725.
- (32) Fazli, M., Almblad, H., Rybtke, M. L., Givskov, M., Eberl, L., and Tolker-Nielsen, T. (2014) Regulation of biofilm formation in *Pseudomonas* and *Burkholderia* species. *Environ. Microbiol.* 16, 1961–1981.
- (33) Weinhouse, H., Sapir, S., Amikam, D., Shilo, Y., Volman, G., Ohana, P., and Benziman, M. (1997) c-di-GMP-binding protein, a new factor regulating cellulose synthesis in *Acetobacter xylinum*. *FEBS Lett.* 416, 207–211.
- (34) Stewart, P. S., and Franklin, M. J. (2008) Physiological heterogeneity in biofilms. *Nat. Rev. Microbiol.* 6, 199.
- (35) Nadell, C. D., Drescher, K., and Foster, K. R. (2016) Spatial structure, cooperation and competition in biofilms. *Nat. Rev. Microbiol.* 14, 589.